Planar infrared binary phase reflectarray

James Ginn,[1,*] Brian Lail,[2] Javier Alda,[3] and Glenn Boreman[1]

[1]*CREOL–The College of Optics and Photonics, University of Central Florida, 4000 Central Florida Boulevard, Orlando, Florida 32816, USA*

[2]*Department of Electrical and Computer Engineering, Florida Institute of Technology, 150 West University Boulevard, Melbourne, Florida 32901, USA*

[3]*Applied Optics Complutense Group, School of Optics, University Complutense of Madrid, Avenue Arcos de Jalón s/n 28037, Madrid, Spain*

**Corresponding author: jcginn@creol.ucf.edu*

Received January 23, 2008; revised February 12, 2008; accepted March 5, 2008; posted March 7, 2008 (Doc. ID 92056); published April 8, 2008

A reflective, binary phase reflectarray is demonstrated in the infrared, at a wavelength of 10.6 μm. The unique aspect of this work, at this frequency band, is that the specific desired phase shift is achieved using an array of subwavelength metallic patches on top of a ground-plane-backed dielectric stand-off layer. This is an alternative to the usual method of constructing a reflective Fresnel zone plate by means of a given thickness of dielectric. This initial demonstration of the reflectarray approach at infrared is significant in that there is inherent flexibility to create a range of phase shifts by varying the dimensions of the patches. This will allow for a multilevel phase distribution, or even a continuous variation of phase, across an optical surface with only two-dimensional lithography, avoiding the need for dielectric height variations. © 2008 Optical Society of America

OCIS codes: 160.3918, 050.5080.

Since the 1930s, metallic, planar Fresnel zone plate (FZP) diffractive lenses and reflectors have been successfully utilized for phase shaping and focusing of electromagnetic radiation [1,2]. The primary benefits of these devices, over their classical counterparts, include reduced volume, lower weight, and cheaper fabrication by removing the need for complicated polishing. Unlike conventional optical elements, however, Soret (binary amplitude) FZP devices exhibit undesirable higher-order foci due to the discrete phase shifts introduced by the binary grading. One method for reducing undesirable foci, while maintaining a planar surface, has been to employ phase correction through index grading [3]. In a graded-index FZP, the number of discrete phase states in the structure is increased through the progressive variation of the index of refraction of a dielectric material contained in each zone of the FZP. Unfortunately, this approach is difficult to implement in the infrared band of the spectrum owing to the lack of practical, low-loss dielectric materials of varying refractive index. Instead, infrared designs have required the implementation of nonplanar dielectric kinoform FZPs [4], which utilize discrete height grading for phase correction or shaping across the zones of the diffractive element. The need for three-dimensional lithography in kinoform FZPs greatly increases the cost and complexity of these devices when compared to binary FZPs.

One potential method to realize a planar, phase-corrected focusing element at infrared is to utilize reflectarray elements in place of the metal or dielectric strips utilized in FZPs. In the microwave and millimeter portion of the spectrum, the microstrip reflectarray has been employed in numerous applications for beam shaping in place of the reflective or refractive elements [5–7]. By definition, the microstrip reflectarray is not a diffractive element, but a quasi-periodic antenna array made up of resonant, subwavelength microstrip elements. By varying the resonant properties of the elements making up the array, it is possible to introduce a graded progressive phase variation upon reflection across the surface of the reflectarray without the need of three-dimensional lithography. The reflectarray also retains many of the benefits of the FZP, including reduced volume, weight, and potentially cheaper fabrication through microlithography. For verification of this potential technology at infrared, a binary phase reflectarray was fabricated for a wavelength of 10.6 μm, and a comparison of modeled behavior and measured results are presented in this Letter.

Reflectarray elements have only recently been demonstrated to achieve selective phase response in the long-wave infrared [8]. The basic resonant element used in development of the 10.6 μm binary phase reflectarray prototype was a metallic patch isolated above a ground plane by a thin dielectric film. By varying the dimensions of the patch along the incident wave's direction of polarization, it is possible to shift the resonant frequency of the element, which in turn changes the phase delay that the wave experiences upon reflection predicted by the Kramers–Kronig relation. Additionally, from antenna theory, the patch element has a broad radiation pattern in the hemisphere above the ground plane. Thus, patches of different sizes can be spatially arranged to allow a physically flat surface to focus an incident phase front by constructive interference at a desired focal point, just like the FZP. By extension, a polarization insensitive design requires both the length and width of the patch to be equal.

Owing to the nonlinear wavelength dependence of the resonant response of the patch elements, it was necessary to model the patch elements using a numerical electromagnetic solver. Ansoft Designer, a

commercially available method of moments solver, was employed to design the reflectarray patch. Dow Corporation's Cyclotene 3022-35, a benzocyclobutene (BCB)-based resin, was used as the stand-off layer owing to the compound's low loss ($k=0.0215$) and small index of refraction at 10.6 μm ($n=1.557$), as well as for ease of deposition through spin coating. A fixed unit cell spacing of 5 μm ($\approx\lambda_0/2$) was employed to minimize grating lobes. Modeling was carried out by varying the size of the patch equally in length and width. In addition, several thicknesses of the BCB film were modeled to determine the optimal patch height above the ground plane. The phase and magnitude response of the patch elements are presented in Figs. 1 and 2, respectively, with the reflected phase shifted to 180°, representing the response of the dielectric and ground plane only (patches of very small size). From modeling and theory, increasing the thickness of the stand-off layer detuned the Q of the resonant element, which allowed for a slower phase transition versus patch size. The slower phase transition reduces the sensitivity of the design to fabrication tolerances, while simultaneously providing less absorption loss as seen in Fig. 2 when thicker stand-off layers are used. From Fig. 1, increasing the thickness of the BCB film resulted in a reduced range of phase variation. However, this limitation can be overcome in future designs through the use of alternative patch geometries such as stub tuned patches or slot loading [9].

With the response of the patch antennas known, an appropriate geometry must be selected for the focusing reflectarray. Binary reflectarrays, for the case of normally incident collimated or spherical wave illumination, follow a layout identical to the Soret FZP. For the binary reflectarray, elements are placed into concentric circular zones with discrete phase steps of 180°. For high f-number configurations, the total number of zones in the reflectarray can be found by the relation

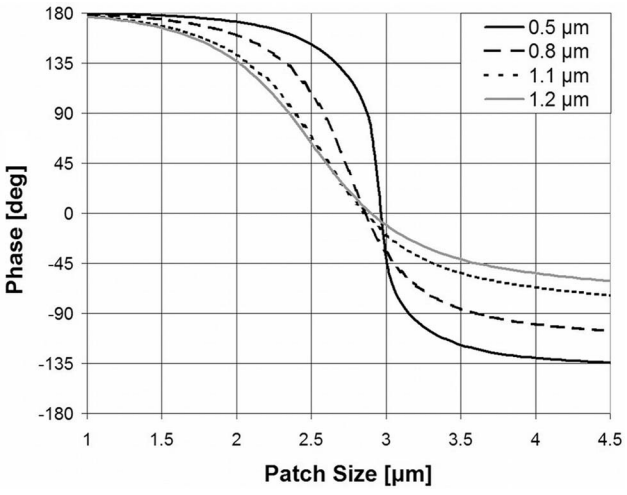

Fig. 1. Modeled phase variation upon reflection for reflectarray elements versus patch dimensions at 10.6 μm. Each line represents a different stand-off layer height.

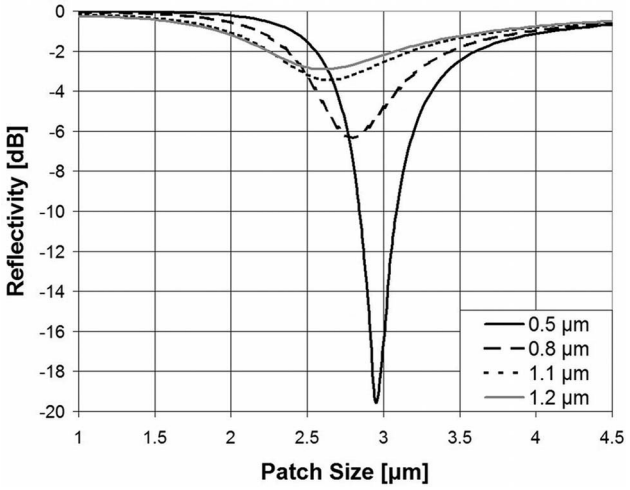

Fig. 2. Modeled power reflectivity for reflectarray elements versus patch dimensions at 10.6 μm. Each line represents a different stand-off layer height.

$$N=\frac{D}{4\lambda f\text{-number}}, \tag{1}$$

where D is the diameter of reflectarray and λ is the design wavelength. Similarly, the distance from the edge of each zone to the center of the structure can be found by the relationship

$$r_n=\sqrt{n\lambda f}, \tag{2}$$

where n is the number of the zone, running from 1 to N, and f is the desired focal length of the design. These relationships can also be adjusted to account for the presence of subzones. Higher-order terms must be included for low f-number designs.

For the prototype, only one discrete phase state of the binary reflectarray was populated with patch elements. The other phase state was simply the combination of the ground plane and the stand-off layer. Based on modeling, a BCB layer thickness of 1.2 μm was chosen to minimize loss, while still providing a reduced volume compared to a ground-plane-backed Soret FZP, which would require a stand-off layer height of approximately $\lambda/4$ or 1.8 μm. The substrate thickness chosen dictated the use of patch elements of dimension 2.83 μm to achieve 180° of phase shift upon reflection, relative to the region without patches. A pattern layout was generated for an f-number 6, 25.4 mm diameter reflectarray with a total of 100 zones and greater than 20×10^6 patch elements. This reflectarray layout is also novel since it is, to our knowledge, the largest known reflectarray ever tested in both number of elements and electrical diameter of the array [10].

With the layout developed, fabrication was carried out using a standard electron beam lithography process to maximize element resolution. The substrate for the reflectarray was selected to be 380 μm thick prime grade silicon wafer to ensure good surface flatness. The ground plane of the reflectarray comprised a 75 nm thick layer of thermally deposited aluminum. Aluminum was chosen in the infrared reflectar-

ray owing to the material's low cost and high conductivity at infrared [11]. Cyclotene 3022-35 was spun onto the surface of the aluminum at a speed of 3500 RPM and baked for 5 min on a hot plate for a cured thickness of approximately 1.2 μm. ZEP 520-A7, a high-resolution electron beam resist, was spun on top of the BCB and the reflectarray pattern was written by a Leica EBPG5000+ electron beam lithography system. After development, 50 nm of aluminum was thermally deposited for the patches and any remaining resist was lifted off. One portion of the array is shown in Fig. 3.

Measurement of the focusing reflectarray was done by imaging the beam profile of a collimated beam reflected off of the reflectarray. Specifically, the beam from a 10.6 μm, 10 W CO_2 laser was initially expanded to a diameter of 25.4 mm collimated beam through a telescope. The collimated beam was then directed by a beam splitter onto the surface of the reflectarray. The reflected focusing beam was projected onto a Spiricon pyroelectric detector array. Determination of the optimal focal point was found by shifting the position of the device under test on a rail to minimize the focused spot size. Figure 4(a) is an image of the fabricated reflectarray element at optimal focus, 152.4 mm away from the camera. Introducing a defocus, as in Fig. 4(b), yields a nearly symmetric blur spot, as expected.

With repeatable modeling, layout generation, fabrication, and testing of the infrared reflectarray now established, continued research will focus on introducing multistep phase shifting and continuous phase gradation in the reflectarray to improve image quality. Future work will also focus on expansion of the reflectarray technology into the midwave infrared and near infrared, and a full characterization of monochromatic and chromatic aberrations.

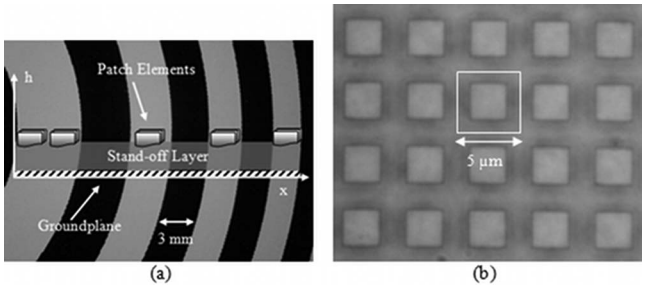

Fig. 3. Visible microscope image of reflectarray rings with (a) layout schematic and (b) patch elements in the rings.

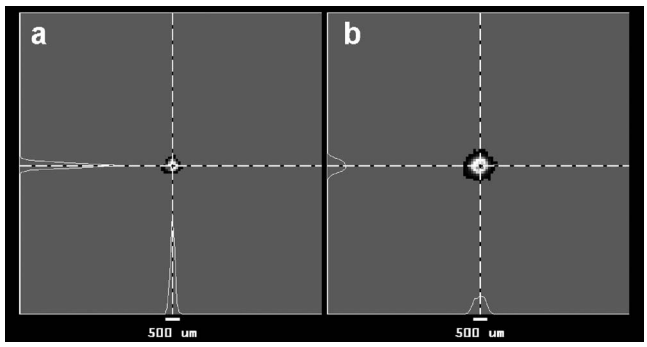

Fig. 4. Reflected beam profiles of reflectarray at (a) optimal focus and (b) reflectarray outside of optimal focus.

This research was supported by a grant from Lockheed Martin Corporation, with additional support from the Florida High Tech Corridor Council.

References

1. J. C. Wiltse, in *Proceedings of IEEE Antennas and Propagation Society International Symposium* (IEEE, 1999), p. 722.
2. G. Z. Jiang and W. X. Zhang, Electromagnetics **19**, 385 (1999).
3. H. D. Hristov, *Fresnel Zones in Wireless Links, Zone Plate Lenses and Antennas* (Artech House, 2000).
4. J. Alda, J. Rico-García, J. López-Alonso, B. Lail, and G. Boreman, Opt. Commun. **260**, 454 (2006).
5. D. Berry, R. Malech, and W. Kennedy, IEEE Trans. Antennas Propag. **11**, 645 (1963).
6. D. M. Pozar, S. D. Targonski, and H. D. Syrigos, IEEE Trans. Antennas Propag. **45**, 287 (1997).
7. F. Tsai and M. Bialkowski, IEEE Trans. Antennas Propag. **51**, 2953 (2003).
8. J. Ginn, B. Lail, and G. Boreman, IEEE Trans. Antennas Propag. **55**, 2989 (2007).
9. D. Cadoret, A. Laisne, and R. Gillard, Microwave Opt. Technol. Lett. **44**, 270 (2005).
10. J. Huang, in *Antenna Engineering Handbook*, J. Volakis, ed. (McGraw Hill, 2007), p. 1.
11. J. Ginn, D. Shelton, J. Tharp, B. Lail, and G. Boreman, in *Proceedings of IEEE Antennas and Propagation Society International Symposium* (IEEE, 2007), p. 4549.